

Document downloaded from:

<http://hdl.handle.net/10251/37860>

This paper must be cited as:

Oroval Cucarella, MDM.; Climent Terol, E.; Coll Merino, MC.; Eritja, R.; Aviñó, A.; Marcos Martínez, MD.; Sancenón Galarza, F.... (2013). An aptamer-gated silica mesoporous material for thrombin detection. *Chemical Communications*. 49(48):5480-5482. doi:10.1039/c3cc42157k.



The final publication is available at

<http://dx.doi.org/10.1039/C3CC42157K>

Copyright Royal Society of Chemistry

# An aptamer-gated silica mesoporous material for thrombin detection

Mar Oroval,<sup>a,b,c</sup> Estela Climent,<sup>a,b,c</sup> Carmen Coll,<sup>a,b,c</sup> Ramón Eritja,<sup>c,d,\*</sup> Anna Aviñó,<sup>c,d</sup> Maria Dolores Marcos,<sup>a,b,c</sup> Félix Sancenón,<sup>a,b,c</sup> Ramón Martínez-Mañez,<sup>a,b,c,\*</sup> Pedro Amorós<sup>e</sup>

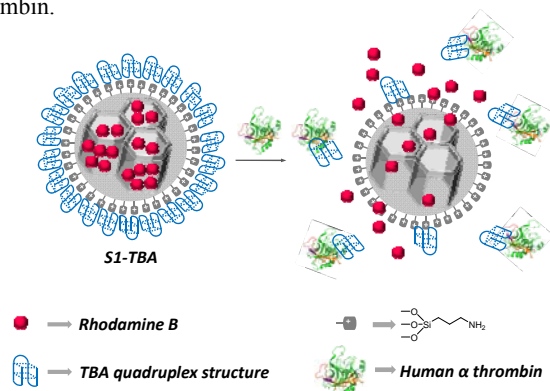
**An aptamer-capped mesoporous material for the selective and sensitive detection of  $\alpha$ -thrombin in human plasma and serum has been prepared and characterised.**

The design of stimuli-responsive nanoscopic gated systems involving biomolecules has recently drawn much attention. In particular, some biomolecules, especially enzymes,<sup>1</sup> have been used as stimuli to uncap gated-scaffolds, whereas others, such as saccharides,<sup>2</sup> antibodies,<sup>3</sup> peptides<sup>4</sup> or DNA,<sup>5</sup> have acted as capping agents. Capped materials have been used mainly in drug delivery applications. However, there are by far fewer examples of their use in sensing.<sup>3</sup> In the latter approach, the carrier system is loaded with a dye and the capped mechanism is designed so that only a target analyte is able to trigger the delivery of the cargo. Among the different biomolecules that could act as caps, aptamers are especially appealing to design gated nanodevices for sensing and targeting applications.<sup>6</sup>

Furthermore,  $\alpha$ -thrombin is a coagulation protein that has many effects on the coagulation cascade and its determination can be used to understand thrombosis and homeostasis processes. This protein, also known as coagulation factor II, is a serine protease that converts soluble fibrinogen (factor I) into insoluble strands of fibrin (factor Ia).<sup>7,8</sup> The concentration of  $\alpha$ -thrombin in blood varies considerably and can be virtually absent in healthy subjects. However in the coagulation process, the concentration of thrombin in blood ranges from nM to low  $\mu$ M levels.<sup>9</sup> Moreover, it is important to detect thrombin in blood serum for clinical and diagnostic applications.<sup>10</sup>

Recently, various aptasensors based on electrochemistry,<sup>11</sup> colorimetry,<sup>12</sup> fluorescence,<sup>13</sup> electrochemiluminescence,<sup>14</sup> and other techniques<sup>15</sup> for thrombin detection have been developed. For instance, electrochemical aptasensors for thrombin detection based on nanoparticle labeling have also been described. For labeling purposes, gold nanoparticles,<sup>16</sup> quantum dots<sup>17</sup> or carbon nanotubes<sup>18</sup> have been widely used. One of the most commonly used aptamers in the development of thrombin aptasensors is the 15-mer DNA aptamer d(5'-GGT TGG TGT GGT TGG-3'), also known as thrombin-binding aptamer (TBA),<sup>19</sup> which is able to bind selectively onto exosite I thrombin (fibrinogen-binding sites) with a high specificity versus other substances.<sup>20</sup>

Despite the above examples, as far as we know, the use of TBA gated-hybrid mesoporous materials to recognize thrombin has not yet been reported. By taking these facts into account, this work presents a new hybrid gated material for the fluorometric detection of  $\alpha$ -thrombin. Based on our experience in the field of bio-gated hybrid materials for sensing applications<sup>21</sup> we report herein the preparation of an aptamer-gated silica mesoporous supports for the selective and sensitive fluorogenic signaling of  $\alpha$ -thrombin.



**Scheme 1.** Schematic representation of the gated material **S1** functionalised with 3-aminopropyltriethoxysilane and capped with a TBA aptamer in the quadruplex state (**S1-TBA**). The delivery of the entrapped guest (rhodamine B) is observed in the presence of  $\alpha$ -thrombin.

Scheme 1 shows the proposed paradigm for thrombin detection using capped mesoporous materials. MCM-41 mesoporous nanoparticles (diameter of ca. 100 nm) were selected as inorganic scaffolds and pores were loaded with a fluorophore (rhodamine B). Then the external surface of the loaded support was functionalised with 3-aminopropyltriethoxysilane (APTS) (solid **S1**). Aminopropyl moieties are partially charged at a neutral pH and should display electrostatic interactions with the negatively charged TBA aptamer. Addition of TBA yielded the final capped hybrid material **S1-TBA**. Specifically for the preparation of the gated material **S1-TBA**, 1.5 mg of **S1** were suspended in 1.5 mL of simulated human blood plasma (pH 7.25).<sup>22</sup> Then, 60  $\mu$ l of TBA (28  $\mu$ M) were added to 150  $\mu$ l of the **S1** suspension. The final **S1-TBA** solid was isolated by centrifugation and washed with 300  $\mu$ l of simulated human blood plasma to eliminate the residual dye and the free TBA.

**S1** was characterised by standard procedures. The X-ray pattern of **S1** shows the mesoporous characteristic (100) peak diffraction, indicating that the loading process with the dye and the further functionalisation with APTS did not damage the mesoporous scaffolding (see Figure S2). The presence of the mesoporous structure in the final functionalised solids is also clearly observed from the TEM analysis (see Figure S2). The N<sub>2</sub> adsorption-desorption isotherms of the calcined MCM-41 nanoparticles (Figure S3) shows an adsorption step with an

<sup>a</sup>Centro de Reconocimiento Molecular y Desarrollo Tecnológico (IDM), Unidad Mixta Universidad Politécnica de Valencia - Universidad de Valencia, Spain.

<sup>b</sup>Departamento de Química, Universidad Politécnica de Valencia, Camino de Vera s/n, 46022, Valencia, Spain. E-mail: rmaez@qim.upv.es

<sup>c</sup>CIBER de Bioingeniería, Biomateriales y Nanomedicina (CIBER-BBN)

<sup>d</sup>Institute for Advanced Chemistry of Catalonia (IQAC), CSIC, Jordi Girona 18-26, E-08034 Barcelona, Spain.

<sup>e</sup>Institut de Ciència dels Materials (ICMUV), Universitat de Valencia, P.O. Box2085, E-46071 Valencia, Spain

† Electronic Supplementary Information (ESI) available: experimental details, synthesis, characterisation and sensing procedures. See <http://dx.doi.org/10.1039/b000000x/>

intermediate  $P/P_0$  value (0.1–0.3). From this curve, a pore volume of  $0.84 \text{ cm}^3 \text{ g}^{-1}$  was calculated by the BJH model on the adsorption branch of the isotherm. The application of the BET model resulted in a value for the total specific surface area of  $1066.8 \text{ m}^2 \text{ g}^{-1}$ . From the XRD, porosimetry and TEM measurements, a pore diameter of 2.57 nm was determined. The  $\text{N}_2$  adsorption-desorption isotherm of **S1** is typical of mesoporous systems with filled mesopores (see Figure S3), with the  $\text{N}_2$  volume adsorbed and a surface area ( $77 \text{ m}^2 \text{ g}^{-1}$ ) significantly decreased.

The dye and APTS contents on solid **S1** were determined by elemental analysis and thermogravimetric studies, and amounted to 0.092 and  $1.65 \text{ mmol g}^{-1}$  solid, respectively. Additionally, the TBA content in solid **S1-TBA** was determined by using aptamer TBA-flu ( $5'$ -GGT TGG TGT GGT TGG-fluorescein- $3'$ ), which is similar to TBA, but is functionalised with a fluorescein dye. By following the decreased absorbance of TBA-flu in the solution after the capping process and by monitoring the TBA-flu release in the uncapping experiments (see SI for details), we were able to calculate a TBA content of  $0.016 \text{ mmol g}^{-1}$  solid.

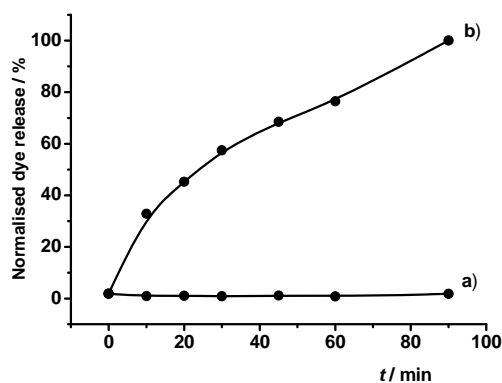


**Figure 1.** Release profile of rhodamine B from solid **S1-TBA** in the absence (a) and presence (b) of  $\alpha$ -thrombin ( $2.89 \mu\text{M}$ ) in simulated human blood plasma (pH 7.25).

In order to investigate the gating properties of **S1-TBA**,  $150 \mu\text{g}$  of **S1-TBA** were suspended in  $1.5 \text{ mL}$  of simulated human blood plasma and the suspension was divided into two fractions. The first fraction was diluted with  $286 \mu\text{L}$  of Milli-Q water, whereas the second one was treated with  $286 \mu\text{L}$  of an aqueous solution containing  $2.89 \mu\text{M}$  of  $\alpha$ -thrombin. In both cases, suspensions were stirred for 90 minutes at  $37^\circ\text{C}$  and at certain times, intervals fractions were taken and centrifuged to remove the solid. Dye delivery at a certain time was then measured by the fluorescence emission of rhodamine in the solution at  $572 \text{ nm}$  ( $\lambda_{\text{exc}} 555 \text{ nm}$ ). The delivery kinetics profile of rhodamine B in the presence and absence of target protein  $\alpha$ -thrombin is displayed in Figure 1. In the absence of  $\alpha$ -thrombin (curve a), solid **S1-TBA** showed a negligible dye release, indicating tight pore closure. The delivery of the dye was induced when  $\alpha$ -thrombin was present in the solution due to the displacement of the aptamer from the nanoparticles as a result of aptamer-thrombin recognition (curve b). After 60 minutes, ca. 80% of delivery was reached (31% of the total adsorbed rhodamine B in solid **S1-TBA**).

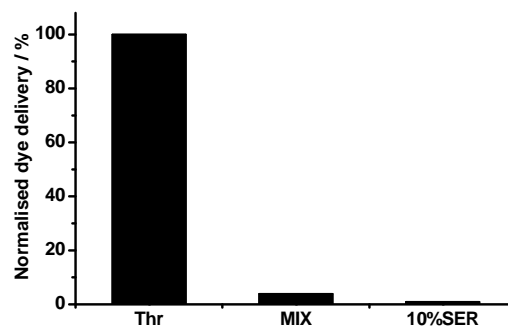


**Figure 2.** Release of rhodamine B from **S1-TBA** in accordance with the concentration of  $\alpha$ -thrombin added (after 60 min of reaction) in simulated human blood plasma (pH 7.25).

Following a similar procedure, the delivery of rhodamine B from **S1-TBA** took place in accordance with the amount of  $\alpha$ -thrombin; the results are shown in Figure 3. As seen, the delivered cargo was proportional to the  $\alpha$ -thrombin concentration, which is in agreement with the uncapping protocol detailed above. Maximum delivery was observed at an  $\alpha$ -thrombin concentration of  $1700 \text{ nM}$ . Finally, a limit of detection of  $2 \text{ nM}$  ( $3\sigma$ ) of  $\alpha$ -thrombin was observed. One special feature of using gated materials for sensing applications is that it separates the recognition protocol (in our case, TBA-protein pair formation) from the signaling event, which means that sensing is independent of the stoichiometry of the host-guest complex, and sometimes, signal enhancement features are displayed. In our particular case, one molecule of  $\alpha$ -thrombin was able to deliver ca. 115 molecules of dye at low  $\alpha$ -thrombin concentrations (ca.  $4 \text{ nM}$ ), which is a remarkable sign of signal amplification.

The *in vitro* characterisation of the nanodevice suggests that **S1-TBA** nanomaterial is sensitive to the presence of  $\alpha$ -thrombin. Moreover, in order to study the possible application in the detection of  $\alpha$ -thrombin in biological samples, **S1-TBA** was tested using commercially available human serum (from human male AB plasma). In a first step, the tolerance of the solid to human serum was studied by suspending  $1 \text{ mg}$  of **S1-TBA** in  $1 \text{ mL}$  of serum diluted with PBS (40, 20, 10 and 5%). From these measurements a 10% serum dilution showed the best response with a limit of detection as low as  $4 \text{ nM}$  of  $\alpha$ -thrombin ( $3\sigma$ ; see Figure S4 and the experimental details in the SI). In a second step, and in order to verify the feasibility of the developed method, we prospectively used solid **S1-TBA** to determine  $\alpha$ -thrombin in human serum. For this purpose, and in a typical experiment, human serum samples were spiked with 75, 150 and  $300 \text{ nM}$  of  $\alpha$ -thrombin, respectively. Samples were diluted with PBS for a final amount of 10%, and the human  $\alpha$ -thrombin contents were determined with **S1-TBA** material by the addition standard method. The obtained results are shown in Table S4. Remarkable recoveries in the range of 91-120% of thrombin were achieved.

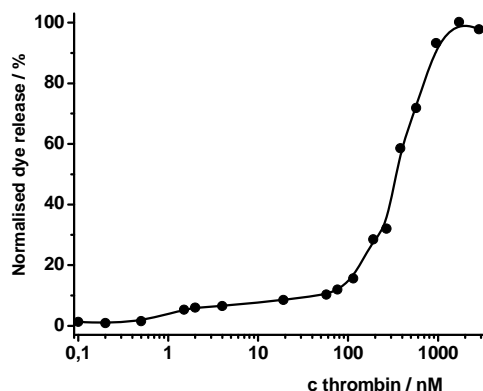


**Figure 3.** Fluorescence of rhodamine B released from **S1-TBA** suspensions (in PBS containing 10% human serum) in the presence of  $\alpha$ -thrombin (56 nM), and a mixture of OVA and BSA (56 nM) after 15 minutes of the addition. For comparative purposes, the release of rhodamine B from the **S1-TBA** suspensions in PBS containing 10% human serum is also shown.

In order to further investigate the selectivity of the **S1-TBA** material, control release experiments were carried out in the presence of other non specific binding proteins (OVA and BSA). In particular, the PBS containing 10% human serum was spiked with 56 nM of OVA and BSA and rhodamine B released after 15 min was measured. Figure 3 shows that a mixture of OVA and BSA was unable to induce the uncapping of pores, which reinforces the selective thrombin-TBA interaction as the mechanism of the fluorogenic response observed.

In conclusion, we have prepared an aptamer-gated delivery system (**S1-TBA**) for the fluorogenic detection of thrombin. The sensing mechanism arises from the high affinity between an aptamer (TBA) and its target protein ( $\alpha$ -thrombin). *In vitro* studies with **S1-TBA** showed a limit of detection of 2 nM ( $3\sigma$ ) for  $\alpha$ -thrombin. In addition, the hybrid nanomaterial allowed accurate  $\alpha$ -thrombin detection in human serum diluted with PBS, also with high sensitivity (limit of detection of 4 nM ( $3\sigma$ )). The method, based on a simple competitive procedure, is undemanding and suggests that the use of aptamers can be a suitable approach to develop gated nanoparticles for simple chromo-fluorogenic assays for a wide range of bio-applications.

The authors thank the Spanish Government (project MAT2012-38429-C04-01, CTQ2010-20541) the Generalitat Valenciana (project PROMETEO/2009/016) and the CIBER-BBN for their support.

## References

- 1 a) K. Patel, S. Angelos, W. R. Dichtel, A. Coskun, Y. -W. Yang, J. I. Zink, J. F. Stoddart, *J. Am. Chem. Soc.*, **2008**, *130*, 2382. b) A. Schlossbauer, J. Kecht, T. Bein, *Angew. Chem. Int. Ed.*, **2009**, *48*, 3092. c) A. Bernardos, E. Aznar, M. D. Marcos, R. Martínez-Mañez, F. Sancenón, J. Soto, J. M. Barat, P. Amorós, *Angew. Chem. Int. Ed.*, **2009**, *48*, 5884. d) C. Park, H. Kim, S. Kim, C. Kim, *J. Am. Chem. Soc.*, **2009**, *131*, 16614. e) P. D. Thornton, A. Heise, *J. Am. Chem. Soc.*, **2010**, *132*, 2024.
- 2 A. Bernardos, L. Mondragón, E. Aznar, M. D. Marcos, R. Martínez-Mañez, F. Sancenón, J. Soto, J. M. Barat, E. Pérez-Payá, C. Guillem, P. Amorós, *ACS Nano*, **2010**, *4*, 6353.

- 3 a) E. Climent, A. Bernardos, R. Martínez-Mañez, A. Maquieira, M. D. Marcos, N. Pastor-Navarro, R. Puchades, F. Sancenón, J. Soto, P. Amorós, *J. Am. Chem. Soc.* **2009**, *131*, 14075. b) E. Climent, R. Martínez-Mañez, A. Maquieira, F. Sancenón, M. D. Marcos, E. M. Brun, J. Soto, P. Amorós, *Chem. Open* **2012**, *1*, 251. c) E. Climent, D. Gröninger, M. Hecht, M. A. Walter, R. Martínez-Mañez, M. G. Weller, F. Sancenón, P. Amorós, and K. Rurack, *Chem. Eur. J.* **2013**, DOI: 10.1002/chem.201300031.
- 4 a) C. Coll, L. Mondragón, R. Martínez-Mañez, F. Sancenón, M. D. Marcos, J. Soto, P. Amorós, E. Pérez-Payá, *Angew. Chem. Int. Ed.*, **2011**, *50*, 2138. b) F. Porta, G. E. M. Lamers, J. I. Zink, A. Kros, *Phys. Chem. Chem. Phys.*, **2011**, *13*, 9982.
- 5 a) A. Schossbauer, S. Warncke, P. M. E. Gramlich, J. Kecht, A. Manetto, T. Carell, T. Bein, *Angew. Chem. Int. Ed.*, **2010**, *49*, 4734. b) Y. Zhang, Q. Yuan, T. Chen, X. Zhang, Y. Chen, W. Tan, *Anal. Chem.*, **2012**, *84*, 1956.
- 6 a) C. -L. Zhu, C. -H. Lu, X. -Y. Song, H. -H. Yang, X. -R. Wang, *J. Am. Chem. Soc.*, **2011**, *133*, 1278. b) V. C. Özalp, T. Schäfer, *Chem. Eur. J.*, **2011**, *17*, 9893. c) L. Gao, Y. Cui, Q. He, Y. Yang, J. Fei, J. Li, *Chem. Eur. J.* **2011**, *17*, 13170. d) X. B. Fu, F. Qu, N. B. Li, H. Q. Luo, *Analyst* **2012**, *137*, 1097.
- 7 C. A. Holland, A. T. Henry, H. C. Whinna, F.C. Church, *FEBS Lett.* **2000**, *484*, 87.
- 8 L. Francois, F.W. David, *Physiol. Rev.*, **1954**, *34*, 722.
- 9 M.A. Shuman, P.W. Majerus, *J. Clin. Invest.* **1976**, *58*, 1249.
- 10 a) J. Zheng, G.-F. Chen, P.-G. He, Y.-Z. Fang, *Talanta*, **2010**, *80*, 1868. b) Y. Wang, X. He, K. Wang, X. Ni, J. Su, Z. Chen, *Biosens. Bioelectron.* **2011**, *26*, 3536.
- 11 a) P.L. He, L. Shen, Y.H. Cao, D.F. Li, *Anal. Chem.* **2007**, *79*, 8024. b) J. Zhao, Y. Zhang, H. Li, Y. Wen, X. Fan, F. Lin, L. Tan, S. Yao, *Biosens. Bioelectron.* **2011**, *26*, 2297.
- 12 a) C.-K. Chen, C.-C. Huang, H.-T. Chang, *Biosens. Bioelectron.*, **2010**, *25*, 1922. b) T. Li, E. Wang, S. Dong, *Chem. Commun.* **2008**, 3654.
- 13 a) H.X. Chang, L.H. Tang, Y. Wang, J. H. Jiang, J.H. Li, *Anal. Chem.* **2010**, *82*, 2341. b) K. A. Edwards, Y. Wang, A. J. Baeumner, *Anal. Bioanal. Chem.* **2010**, *398*, 2645.
- 14 a) X.-B. Yin, Y.-Y. Xin, Y. Zhao, *Anal. Chem.*, **2009**, *81*, 9299. b) L. Fang, Z. Lü, H. Wei, E. Wang, *Anal. Chim. Acta*, **2008**, *628*, 80. c) J. Wang, Y.-Y. Shan, W. Zhao, J.-J. Xu, H.-Y. Chen, *Anal. Chem.* **2011**, *83*, 4004.
- 15 a) Q. Zhao, X.F. Lu, C.-G. Yuan, X.-F. Li, X.C. Le, *Anal. Chem.*, **2009**, *81*, 7484. b) J. Hu, P.-C. Zheng, J.-H. Jiang, G.-L. Shen, R.-Q. Yu, G.-K. Liu, *Anal. Chem.* **2009**, *81*, 87.
- 16 C.F. Ding, Y. Ge, J. -M. Lin, *Biosens. Bioelectron.*, **2010**, *25*, 1290.
- 17 a) C.F. Ding, Y. Ge, S.S. Zhang, *Chem. Eur. J.*, **2010**, *16*, 10707. b) Y. H. Tennico, D. Hutanu, M. T. Koesdjojo, C. M. Bartel, V. T. Remcho, *Anal. Chem.*, **2010**, *82*, 5591.
- 18 M.M. Teresa, Y.-C. Tseng, N. Ormategui, I. Loinaz, R. Eritja, J. Bokor, *Nano Lett.*, **2009**, *9*, 530.
- 19 L. C. Bock, L. C. Griffin, J. A. Latham, E. H. Vermaas, J. J. Toole, *Nature*, **1992**, *355*, 564.
- 20 a) W. Bode, D. Turk, A. Karshikov, *Protein Sci.*, **1992**, *1*, 426. b) M.T. Stubbs, W. Bode, *Thromb. Res.*, **1993**, *69*, 1.
- 21 E. Climent, R. Martínez-Mañez, F. Sancenón, M. D. Marcos, J. Soto, A. Maquieira, P. Amorós, *Angew. Chem. Int. Ed.* **2010**, *49*, 7281.
- 22 M. R. C. Marques, R. Loebenberg, M. Almukainzi, *Dissolution Technologies*, **2011**, *18*, 15.